Available online at www.sciencedirect.com
ScienceDirect
ELSEVIER
Journal of the European Ceramic Society 28 (2008) 401–406
www.elsevier.com/locate/jeurceramsoc

Kinetics of alumina segregation in mullite ceramics

P. Fielitz [a,*], G. Borchardt [a], P. Mechnich [b], M. Schmücker [b]

[a] *Institut für Metallurgie, Technische Universität Clausthal, Robert-Koch-Str. 42, Germany*
[b] *Institut für Werkstoff-Forschung, Deutsches Zentrum für Luft- und Raumfahrt, Porz-Wahnheide, Linder Höhe, D-51147 Köln, Germany*

Available online 1 May 2007

Dedicated to Prof. Hartmut Schneider on the occasion of his 65th birthday.

Abstract

Dense polycrystalline mullite was equilibrated for 6 h in air at 1800 °C and then quenched to room temperature. During subsequent annealing at 1600 °C a gradual decrease of the Al_2O_3 concentration in the grains occurs which approaches an equilibrium concentration after about 100 h annealing time. A simplified model of spherical grains of uniform size is applied to describe the observed kinetics of the Al_2O_3 concentration decrease in the mullite grains. This model allows to determine a chemical diffusion coefficient of Al_2O_3 from the measured kinetics data. This chemical diffusion coefficient of Al_2O_3 is compared to the ambipolar diffusion coefficient of Al_2O_3 calculated from our tracer diffusivity data in single crystalline 2/1-mullite. The resulting thermodynamic factor is in reasonable agreement with the value calculated from literature data for mullite formation in a solid state reaction.

Keywords: Mullite; Alumina segregation kinetics

1. Introduction

Mullite is a promising and widely studied material for high temperature applications. The composition of mullite can be expressed as $Al^{VI}_2(Al^{IV}_{2+2x}Si_{2-2x})O_{10-x}$ with x ranging between 0.18 and 0.88.[1] Typical mullite compositions, however, are between $x = 0.25$ ($3Al_2O_3 \cdot 2SiO_2$, 3/2-mullite) and $x = 0.4$ ($2Al_2O_3 \cdot 1SiO_2$, 2/1-mullite). As a matter of principle most high temperature effects of mullite ceramics (diffusional creep, grain growth, reconstructive transformations, etc.) are controlled by the mobility of the relevant atomic species. Thus, for a deeper insight into diffusion-related processes we have carried out comprehensive tracer diffusion experiments (^{18}O, ^{30}Si, ^{26}Al) within the last few years.[2–4] Recently, we have presented a consistent reaction model for the solid state formation of mullite basing upon the tracer diffusivity data.[5] The aim of the present paper is to analyse compositional variations of mullite crystals in the light of the diffusivity of the involved atomic species. The change of mullite composition and related segregation of silica or alumina, respectively, is a well known phenomenon that occurs during high temperature processing or application. (Throughout this paper the term "segregation" comprises any change of the concentrations of the constituent elements in the mullite grains which leads to subsequent precipitation of alumina (or silica) at the grain boundaries.) The concentration change is due to the fact that the stability field of mullite is sloped towards Al_2O_3 at temperatures higher than 1600 °C.[6] As a consequence, if polycrystalline mullite with an overall composition of $Al_2O_3/SiO_2 = 3/2$ is fired above 1600 °C the composition of individual mullite grains gradually becomes richer in Al_2O_3 going along with the formation of silica-rich melt. During cooling down, the melt typically forms a glassy phase and hence the corresponding mullite crystals remain supersaturated in Al_2O_3. A different situation exists in ceramics of mullite/α-alumina phase assemblages: preliminary investigations revealed that the mullite composition can shift reversibly, balanced by the amount of coexisting α-Al_2O_3.[7]

2. Experimental

Dense polycrystalline mullite with minor amounts of α-Al_2O_3, typically occurring at mullite triple grain junctions was used as starting material. The ceramic sample was fabricated using a coprecipitated mullite precursor fired at 1700 °C and

* Corresponding author. Tel.: +49 5323 72 2634; fax: +49 5323 72 3184.
E-mail address: peter.fielitz@tu-clausthal.de (P. Fielitz).

0955-2219/$ – see front matter © 2007 Elsevier Ltd. All rights reserved.
doi:10.1016/j.jeurceramsoc.2007.03.014

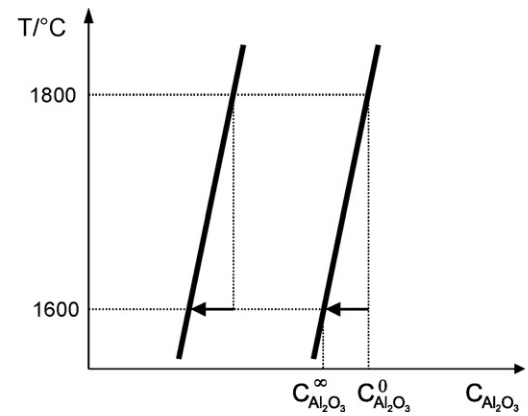

Fig. 1. Schematic representation of the alumina-silica phase diagram to illustrate the reaction path after quenching from 1800 to 1600 °C, where $c_{Al_2O_3}$ is the Al_2O_3 concentration. Solid lines illustrate the stability range of mullite in the alumina-silica phase diagram.

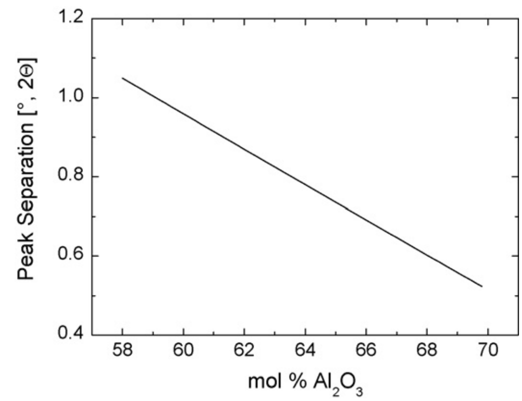

Fig. 2. Separation between (2 5 1) and (5 2 1) diffraction peaks (2Θ, Cu K_α) of mullite as a function of composition.

was subsequently hot isostatically pressed at 1600 °C. A detailed description of the processing of the material is given elsewhere.[8] For our experiments the specimens were fired at 1800 °C for 6 h in air thus leading to significant Al_2O_3 enrichment of the mullite grains ($c^0_{Al_2O_3}$ in Fig. 1). After quenching, the high amount of alumina was frozen in. During subsequent annealing at 1600 °C, the mullite composition gradually approaches equilibrium composition ($c^{\infty}_{Al_2O_3}$ in Fig. 1). The average composition was monitored by X-ray diffractometry making use of the fact that the *a* lattice constant of mullite depends in a linear way on its Al_2O_3 content according to $a = 0.00692m + 7.124$ with *m* as the molar content of Al_2O_3 in mullite and *a* in Å.[1] *b* and *c* axes of mullite, on the other hand, are virtually unaffected by the composition in the interesting region. To ensure high accuracy of relative compositional changes due to the 1600 °C firing steps an identical piece of ceramics was used throughout the annealing procedure. The Al_2O_3 content was determined from the separation between (2 5 1) and (5 2 1) diffraction peaks (Fig. 2). X-ray diffraction was performed using a Siemens D 5000 system equipped with a Cu X-ray tube. The interesting regions of the diffraction pattern were recorded with a step width of 0.01 and 10 s counting time. Average Al_2O_3 contents as a function of annealing history are listed in Table 1. As expected, the alumina content increases with respect to the starting material after firing at 1800 °C and gradually decreases by subsequent annealing at 1600 °C. The absolute composition, however, is poorer in alumina than anticipated from the phase diagram given by Klug et al.[6]

To derive an analytical solution for the observed kinetics of the average Al_2O_3 concentration we consider a simplified model of spherical grains of equal radius *R*. The diffusion equation then becomes[9]:

$$\frac{\partial u(r,t)}{\partial t} = \tilde{D}_{Al_2O_3} \frac{\partial^2 u(r,t)}{\partial r^2} \quad \text{with} \quad u(r,t) = r c_{Al_2O_3}(r,t) \tag{1}$$

where $\tilde{D}_{Al_2O_3}$ is the chemical diffusion coefficient of Al_2O_3, *r* the distance from the centre of the spherical grains and $c_{Al_2O_3}$ is the concentration of Al_2O_3 in the grains.

The reaction path after quenching from 1800 to 1600 °C is illustrated in Fig. 1. Near the grain boundaries ($r \approx R$) the equilibrium concentration, $c^{\infty}_{Al_2O_3}$, will be reached rapidly since the mullite/mullite boundaries act as fast diffusion paths for aluminium and oxygen ions moving towards the segregated α-Al_2O_3 grains. Neglecting the (short) transition time we have the following initial and boundary condition:

$$\begin{aligned} c_{Al_2O_3} &= c^0_{Al_2O_3}, \quad t = 0, \quad 0 < r < R \\ c_{Al_2O_3} &= c^{\infty}_{Al_2O_3}, \quad t > 0, \quad r = R. \end{aligned} \tag{2}$$

Table 1
Average concentration of Al_2O_3 in the mullite grains of as-received ceramics, ceramics fired at 1800 °C, and ceramics subsequently annealed at 1600 °C for various periods

Status of the mullite ceramics	Annealing time at 1600 °C (h)	Concentration of Al_2O_3 (mol%)	x[a]
As received		62.80	0.3145
Fired at 1800 °C, 6 h		63.70	0.3347
Fired at 1800 °C, 6 h and subsequently annealed at 1600 °C	2	63.55	0.3314
	6	63.15	0.3224
	12	63.00	0.3190
	24	62.45	0.3066
	48	62.00	0.2963
	100	61.90	0.2940

[a] In literature mullite composition is often expressed as $Al_{4+2x}Si_{2-2x}O_{10-x}$.

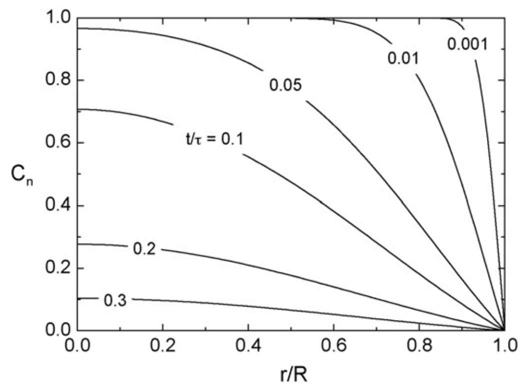

Fig. 3. Normalised radial Al_2O_3 concentration in grains of radius R plotted for different t/τ ratios.

An analytical solution of Eq. (1) respecting these conditions is given by[9]:

$$C_n(r,t)=\frac{c_{Al_2O_3}(r,t)-c^{\infty}_{Al_2O_3}}{c^{0}_{Al_2O_3}-c^{\infty}_{Al_2O_3}}=\sum_{n=1}^{\infty}(-1)^{n+1}\frac{2\sin(n\pi\xi)}{n\pi\xi}\exp\left(-n^2\pi^2\frac{t}{\tau}\right)\quad\text{with}\quad\xi=\frac{r}{R},\qquad \tau=\frac{R^2}{\tilde{D}_{Al_2O_3}} \tag{3}$$

where $C_n(r, t)$ is the normalised radial Al_2O_3 concentration in grains of radius R. In Fig. 3 Eq. (3) is plotted for different t/τ ratios, where τ is a characteristic time constant to achieve the equilibrium concentration, $c^{\infty}_{Al_2O_3}$. To calculate the average Al_2O_3 concentration in the grains we apply the following integration:

$$\bar{c}_{Al_2O_3}(t)=\frac{1}{R}\int_{r=0}^{R}c_{Al_2O_3}(r,t)\,dr \tag{4}$$

which gives for Eq. (3)

$$\bar{C}_n(t)=\frac{\bar{c}_{Al_2O_3}(t)-c^{\infty}_{Al_2O_3}}{c^{0}_{Al_2O_3}-c^{\infty}_{Al_2O_3}}=\sum_{n=1}^{\infty}(-1)^{n+1}\frac{2\,\mathrm{Si}(n\pi)}{n\pi}\exp\left(-n^2\pi^2\frac{t}{\tau}\right)\quad\text{with}\quad \mathrm{Si}(x)\equiv\int_0^x\frac{\sin(t)}{t}\,dt \tag{5}$$

where $\bar{C}_n$ is the normalised average Al_2O_3 concentration. To normalise the average Al_2O_3 concentrations compiled in Table 1 we used the following initial concentration and equilibrium concentration of Al_2O_3 in the grains

$$c^{0}_{Al_2O_3}=63.7\,\text{mol\%};\qquad c^{\infty}_{Al_2O_3}=61.9\,\text{mol\%} \tag{6}$$

where $c^{0}_{Al_2O_3}$ was the Al_2O_3 content after firing at 1800 °C for 6 h and $c^{\infty}_{Al_2O_3}$ is the Al_2O_3 content reached asymptotically after long-term annealing at 1600 °C. Fig. 4 shows a fit of Eq. (5) to our measured normalised average Al_2O_3 concentrations which

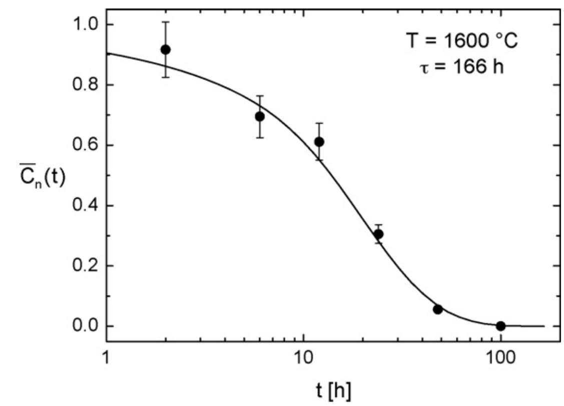

Fig. 4. Fit of Eq. (5) to the experimental data for the normalised average Al_2O_3 concentration.

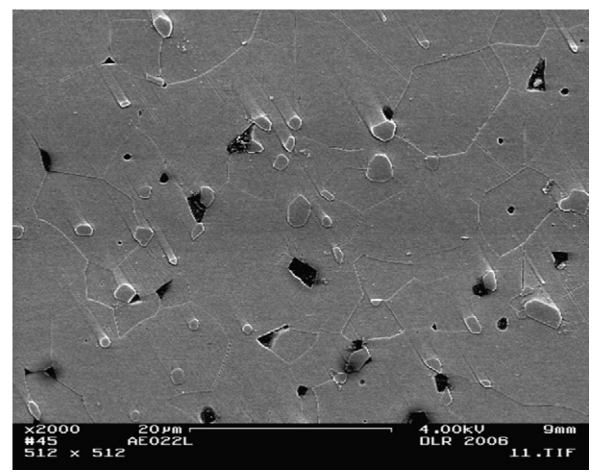

Fig. 5. Microstructure of the mullite ceramics after pre-annealing for 6 h at 1800 °C in air.

yields for the characteristic time constant

$$\tau=\frac{R^2}{\tilde{D}_{Al_2O_3}}=166\,\text{h}\ \text{at}\ T=1600\,^{\circ}\text{C}. \tag{7}$$

The microstructure of the mullite ceramics after pre-annealing for 6 h at 1800 °C in air is shown in Fig. 5. The coarsened microstructure does not change significantly during subsequent annealing at lower temperature (1600 °C). Estimating an average grain radius $R = 5$ µm we can calculate the chemical diffusion coefficient of Al_2O_3 at 1600 °C

$$\tilde{D}_{Al_2O_3}=\frac{R^2}{\tau}=4.2\times10^{-17}\frac{m^2}{s}\ \text{at}\ T=1600\,^{\circ}\text{C}. \tag{8}$$

3. Discussion

Tracer diffusivity studies in single crystalline mullite[2–5] show that silicon is the slowest species compared to oxygen and aluminium. Therefore, we can neglect Si^{4+} ion fluxes and suppose that Al_2O_3 is transported via coupled Al^{3+} and O^{2-} ion fluxes through the single crystalline mullite grains.[5] The two coupled Al^{3+} and O^{2-} ion fluxes can be expressed by a single ambipolar (molecular) flux of Al_2O_3. The associated ambipolar diffusion coefficient, $D_{Al_2O_3}$, of Al_2O_3 is given by (Philibert,[10] p. 244)

$$\frac{1}{D_{Al_2O_3}} = \frac{2}{D_{Al^{3+}}} + \frac{3}{D_{O^{2-}}} \tag{9}$$

where D_i is the self-diffusion coefficient of the ion i (Al^{3+}, O^{2-}) which is related to the random thermal motion of the ions. The chemical diffusion coefficient, $\tilde{D}_{Al_2O_3}$, of Al_2O_3 determined from our alumina segregation experiment is related to the ambipolar diffusion coefficient, $D_{Al_2O_3}$, via the following expression (Philibert,[10] p. 204)

$$\tilde{D}_{Al_2O_3} = D_{Al_2O_3}\Phi \text{ with } \Phi = \frac{d\ln(a_{Al_2O_3})}{d\ln(N_{Al_2O_3})} \tag{10}$$

where Φ is the thermodynamic factor, $a_{Al_2O_3}$ is the activity and $N_{Al_2O_3}$ the mole fraction of Al_2O_3. Correlation factors for self-diffusion are often in the order of 1 (Philibert,[10] p. 98) so that we can calculate the ambipolar diffusion coefficient, $D_{Al_2O_3}$, of Al_2O_3 in a first order approximation from our measured tracer diffusivities.[5] With the experimentally determined (average) chemical diffusion coefficient, $\tilde{D}_{Al_2O_3}$, of Al_2O_3 one calculates a thermodynamic factor of about 6.5 for the performed alumina segregation experiment

$$\Phi = \frac{\tilde{D}_{Al_2O_3}}{D_{Al_2O_3}} = 6.5 \text{ at } T = 1600^\circ\text{C}. \tag{11}$$

To check this value for plausibility, we will derive in the following the thermodynamic factor from literature data. By definition, the differential of the chemical potential of Al_2O_3 is given by[11]:

$$d\mu_{Al_2O_3} = RT\,d\ln(a_{Al_2O_3}) = RT\,d\ln(N_{Al_2O_3}) + RT\,d\ln(\gamma_{Al_2O_3}) \tag{12}$$

where $\gamma_{Al_2O_3}$ is the activity coefficient of Al_2O_3. Defining a differential of the concentration potential of Al_2O_3

$$d\varphi_{Al_2O_3} = RT\,d\ln(N_{Al_2O_3}) \tag{13}$$

the thermodynamic factor can also be expressed by the ratio of both potential differences

$$\Phi = \frac{d\mu_{Al_2O_3}}{d\varphi_{Al_2O_3}}. \tag{14}$$

Eq. (14) will be used for further calculations of the thermodynamic factor. However, as we will see later in the discussion it is, as yet, not possible to calculate an exact value of the thermodynamic factor for our alumina segregation experiment. Therefore, Φ will be estimated using thermodynamic data derived from mullite formation studies performed by Aksay[12] and Aksay and Pask.[13]

3.1. Mullite formation

Aksay[12] and Aksay and Pask[13] used diffusion couples made from sapphire and aluminium-silicate glasses to study the growth kinetics of mullite as an intermediate phase. The thickness of the mullite layer increased linearly with the square root

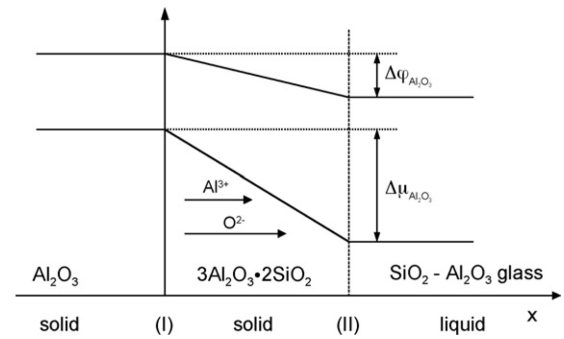

Fig. 6. Schematic representation of the mullite formation reaction. Al_2O_3 is transported through the solid mullite layer by means of intrinsic Al^{3+} and O^{2-} ion fluxes and reacts to 3/2-mullite with SiO_2 from the aluminosilicate melt which is in equilibrium with mullite. The chemical potential difference of Al_2O_3 across the mullite layer, $\Delta\mu_{Al_2O_3}$, is compared to the concentration potential difference, $\Delta\varphi_{Al_2O_3}$, of Al_2O_3 at the interfaces (I) and (II).

of time, indicating that the growth mechanism was diffusion-controlled. A diffusion-controlled mullite formation reaction model was proposed recently[5] to relate the measured parabolic growth constants to tracer diffusivities. The above defined potential differences of Al_2O_3 across the growing mullite layer are illustrated in Fig. 6. The formation of 3/2-mullite from the oxides

$$2SiO_2 + 3Al_2O_3 = Al_6Si_2O_{13} \tag{15}$$

is driven by the chemical potential difference of Al_2O_3 across the mullite layer[5]

$$\Delta\mu_{Al_2O_3} = \frac{\Delta_r G^\circ_{Al_6Si_2O_{13}}}{3} - \frac{2}{3}RT\ln(a^{II}_{SiO_2}) \tag{16}$$

where $a^{II}_{SiO_2}$ is the activity of SiO_2 in the aluminium-silicate glass melt and $\Delta_r G^\circ_{Al_6Si_2O_{13}}$ is the Gibbs energy of formation of 3/2-mullite from the oxides which can be calculated[14,15] from the Gibbs energies of formation from the elements, $\Delta_f G^\circ_i$

$$\Delta_r G^\circ_{Al_6Si_2O_{13}} = \Delta_f G^\circ_{Al_6Si_2O_{13}} - 3\Delta_f G^\circ_{Al_2O_3} - 2\Delta_f G^\circ_{SiO_2} \tag{17}$$

In order to calculate an approximate value of the thermodynamic factor we compare the chemical potential difference, $\Delta\mu_{Al_2O_3}$, of Al_2O_3 with the concentration potential difference, $\Delta\varphi_{Al_2O_3}$, of Al_2O_3

$$\Delta\varphi_{Al_2O_3} = RT\ln\left(\frac{N^{II}_{Al_2O_3}}{N^{I}_{Al_2O_3}}\right) \tag{18}$$

where $N^{I}_{Al_2O_3}$ is the mole fraction of Al_2O_3 at the sapphire/mullite interface (I) and $N^{II}_{Al_2O_3}$ is the mole fraction of Al_2O_3 at the mullite/glass interface (II). The resulting thermodynamic factors for the 3/2-mullite formation reaction at different temperatures are compiled in Table 2 using the experimental data of Aksay and Pask.[13] It turns out that the concentration potential difference is much lower than the chemical potential difference resulting in a thermodynamic factor of about 9. We assume that the scatter of the calculated thermodynamic factors is mainly caused by errors of the measurement of the Al_2O_3 mole fractions at the interfaces.

Table 2
Chemical potential and concentration potential differences of Al_2O_3 and thermodynamic factors calculated by Eqs. (14), (16), and (18)

Experimental data of Aksay et al.[13]						Calculated values		
T (°C)	RT (kJ/mol)	$\Delta_r G^\circ_{Al_6Si_2O_{13}}$ (kJ/mol)	$a^{II}_{SiO_2}$	$N^{II}_{Al_2O_3}$ (mol%)	$N^{I}_{Al_2O_3}$ (mol%)	$\Delta\mu_{Al_2O_3}$ (kJ/mol)	$\Delta\varphi_{Al_2O_3}$ (kJ/mol)	Φ
1678	16.2	−33.8	0.93	58.6	62.7	−10.5	−1.10	9.5
1753	16.8	−35.3	0.85	58.6	62.7	−9.91	−1.14	8.7
1813	17.3	−36.5	0.70	59.9	62.7	−7.96	−0.79	10.1

The activity of SiO_2 at phase boundary II, $a^{II}_{SiO_2}$, was approximated by the mole fraction of SiO_2 in the aluminosilicate melt. The Gibbs energy change, $\Delta_r G^\circ_{Al_6Si_2O_{13}}$, for the formation of 3/2-mullite from the oxides was calculated with Eq. (17) using tabulated thermochemical data.[14]

3.2. Alumina segregation

Based on the results for the mullite formation experiment we are now able to estimate the thermodynamic factor of our alumina segregation experiment. During our experiment the Al_2O_3-supersaturated mullite grains deplete in Al_2O_3 in favour of the coexisting α-Al_2O_3 phase. The driving force for the segregation of Al_2O_3 at 1600 °C is the chemical potential gradient of Al_2O_3 between grain centers and grain boundaries. The gradient is maximum at the beginning of the annealing experiment and will approach zero asymptotically after long annealing times. The maximum concentration potential difference can be calculated from the initial concentration and the equilibrium concentration of Al_2O_3 in the grains (see Eq. (6))

$$\Delta\varphi^{max}_{Al_2O_3} = RT \ln\left(\frac{c^{\infty}_{Al_2O_3}}{c^{0}_{Al_2O_3}}\right) = -0.45\,\text{kJ/mol} \tag{19}$$

Obviously, this value is about half the value calculated for the mullite formation reaction (see Table 2). This means, the thermodynamic factor is about 9 (mean value of Table 2) provided the amount of the Gibbs energy of the Al_2O_3 segregation from the mullite grains and its precipitation at the grain boundaries

$$Al_6Si_2O_{13} = Al_{6-2\delta}Si_2O_{13-3\delta} + \delta Al_2O_3 \tag{20}$$

is about a factor of two lower than the Gibbs energy of the mullite formation from the oxides (Eq. (15)). As the value of the exact Gibbs energy is not known for the segregation reaction (20) one can assume that the Gibbs energy of this reaction is significantly lower (by a factor of the order $\delta/3 \approx 10^{-2}$) than the Gibbs energy of the formation reaction. Therefore, it can be expected that a thermodynamic factor of 9 is the upper limit (in the given temperature range). Thus, we have a criterion to check our experimental data for self-consistence.

A thermodynamic factor of 6.5 was calculated for the performed alumina segregation experiment derived from the ratio of ambipolar to chemical diffusivity data (see Eq. (11)). This value is indeed lower than the upper limit of 9, so that our data sets of two different independent experiments (the former tracer experiments and the recent segregation experiment) are consistent.

4. Summary

We have studied the kinetics of segregation of Al_2O_3 from alumina-rich mullite grains at 1600 °C. Previous tracer diffusivity studies showed that the diffusivity of ^{30}Si in single crystalline mullite is much lower compared to the diffusivities of ^{26}Al and ^{18}O, which are almost equal.[5] Because of this observation we assume that the segregation kinetics of Al_2O_3 from the mullite grains is controlled by the diffusivities of aluminium ions and oxygen ions which can be expressed by an ambipolar diffusion coefficient of Al_2O_3 (see Eq. (9)).

A simplified model of spherical grains of equal radius was applied to derive an analytical solution for the kinetics of the segregation of Al_2O_3 from the mullite grains towards the respective grain boundaries. This model allowed to evaluate a chemical diffusion coefficient of Al_2O_3 from the experimental kinetics data. Neglecting correlation effects for the tracer diffusion we calculated the ambipolar diffusion coefficient of Al_2O_3 in a first order approximation by our measured tracer diffusivities.[5] Comparing the ambipolar diffusion coefficient and the chemical diffusion coefficient of Al_2O_3 a thermodynamic factor of 6.5 was calculated for our experimental conditions. On the basis of literature data we could further demonstrate that thermodynamic factors below 9 are plausible, thus supporting the assumption that only the (fairly similar) mobilities of Al^{3+} and O^{2-} ions control the segregation of alumina from alumina-rich mullite grains. The simplified spherical grain model seems to be fully sufficient for the mathematical description of the diffusion conditions in our segregation experiment.

Acknowledgements

We are indebted to Prof. Hartmut Schneider for his interest in our work and his continuous encouragement. Financial support from Deutsche Forschungsgemeinschaft (DFG) is gratefully acknowledged.

References

1. Fischer, R. X., Schneider, H. and Voll, D., Formation of aluminium-rich 9:1 mullite and its transformation to low alumina mullite upon heating. *J. Eur. Ceram. Soc.*, 1996, **16**, 109–113.
2. Fielitz, P., Borchardt, G., Schmücker, M., Schneider, H., Wiedenbeck, M., Rhede, D. *et al.*, Secondary ion mass spectroscopy study of oxygen-18 tracer diffusion in 2/1-mullite single crystals. *J. Am. Ceram. Soc.*, 2001, **84**(12), 2845–2848.
3. Fielitz, P., Borchardt, G., Schmücker, M. and Schneider, H., Silicon tracer diffusion in single crystalline 2/1-mullite measured by SIMS depth profiling. *Phys. Chem. Chem. Phys.*, 2003, **5**(11), 2279–2282.
4. Fielitz, P., Borchardt, G., Schmücker, M. and Schneider, H., Al-26 diffusion measurement in 2/1-mullite by means of secondary ion mass spectrometry. *Solid State Ionics*, 2006, **177**(5–6), 493–496.

5. Fielitz, P., Borchardt, G., Schmücker, M. and Schneider, H., A diffusion-controlled mullite formation reaction model based on tracer diffusivity data for aluminium, silicon and oxygen. *Philos. Mag.*, 2007, **87**, 111–127.
6. Klug, F. J., Prochazka, S. and Doremus, R. H., Alumina-silica phase diagram in the mullite region. *J. Am. Ceram. Soc.*, 1987, **70**, 750–759.
7. Thom, M. and Schmücker, M., unpublished results.
8. Kanka, B. and Schneider, H., Sintering mechanisms and microstructural development of coprecipitated mullite. *J. Mater. Sci.*, 1994, **29**, 1239–1249.
9. Crank, J., *The Mathematics of Diffusion* (*2nd ed.*). Oxford University Press, Oxford, 1975.
10. Philibert, J., *Atom Movements: Diffusion and Mass Transport in Solids*. Éditions de Physique, Les Ulis, 1991.
11. Schmalzried, H., *Solid State Reactions* (*2nd ed.*). Verlag Chemie, Weinheim, 1981.
12. Aksay, I.A., *Diffusion and Phase Relationship Studies in the Alumina-Silica System*. PhD thesis, University of California, Berkeley, 1973.
13. Aksay, I. A. and Pask, J. A., Stable and metastable equilibria in the system SiO_2–Al_2O_3. *J. Am. Ceram. Soc.*, 1975, **58**(11/12), 507–512.
14. Barin, I., *Thermochemical Data of Pure Substances. Part I + II*. VCH Publishers, Weinheim, 1989.
15. Chase Jr., M. W., Davies, C. A., Downey Jr., J. R., Frurip, D. J., McDonald, R. A. and Syverud, A. N., *JANAF Thermochemical Tables* (*3rd ed.*). ACS, AIP, NBS, New York, 1986.